Bachelor Thesis

Development of an Upconverting Nanoparticles Quantum Yield Measurement System

Meng Li

Thesis submitted for the degree of Bachelor of Science
Project duration: Jan-May 2016, half-time equivalent
LRAP 520 (2016)

LUND
UNIVERSITY

Supervisor: Monirehalsadat Mousavi
Co-Supervisor: Stefan Andersson Engels
Department of Physics
Atomic Physics Division
Biophotonics Group
May 2016

Abstract

Fluorescence imaging is a growing biomedical technique; it can be used to localize the luminescent biomarkers inside the tissue. Lanthanide-doped upconverting nanoparticles (UCNPs) are promising luminescent probes for multiple applications in biophotonics. They allow acquiring autofluorescence-free recordings with high spatial resolution. However, upconverting nanoparticles have a low quantum yield, especially at low excitation power densities. In this thesis, an upconverting nanoparticles quantum yield measurement system is developed, the upconverting nanoparticles used are the sodium yttrium tetra fluoride doped with thulium and ytterbium ions, $NaYF_4$: Yb^{3+},Tm^{3+}. The quantum yield for UCNPs is dependent on the excitation power density. A well-characterized dye, DY-781, with a known quantum yield of 11.9%, is used as the reference dye in these measurements. Upconverting nanoparticles quantum yield is then obtained by using a comparative method. At the balance point, half way to completely saturating the excitation, the power density equals 3214 $mWcm^{-2}$, and the nanoparticles have a quantum yield of approximately 0.33%. The quantum yield of upconverting nanoparticles can be presented as a function of the excitation power density, and the values for maximum attainable quantum yield is estimated to be 0.69%. The setup is successful for obtaining the saturation of thulium-doped upconverting nanoparticles as they saturate at low power densities.

Acknowledgments

Firstly, I would like to express my sincere gratitude to my main supervisor Ari, Monirehalsadat Mousavi. Thank you very much for your constant help and your encouragement. It was my first time experiencing thesis work and a biophotonic topic. I always came to you when I ran into trouble, and you were always there with patient and detailed explanations. It was your guidance and encouragement that allowed me to finish this thesis.

I would like to thank my co-supervisor, Stefan Andersson-Engels. Thank you so much for offering me the opportunity to take this thesis work; it has always been my dream to become a biophotonic researcher in tumor treatment fields. Your advance and help on my thesis work were valuable. Both you and Ari would stay late just to help me to fix the setup; I appreciated that so much. Doing research together with you and Ari was such an amazing and precious experience; I had so much fun during this thesis work.

I would also like to acknowledge Marco Kraft, a Ph.D. student from Bam. You helped me so much through the process of data collecting, data evaluation, and writing the thesis. And thank you so much for the help with LabVIEW, your modifications allow the data collecting work becomes easier and more precise. I hope you had fun during the time you were in Lund.

Special thanks to Åke Johansson. Welding was great fun, and you were very patient teaching me how to do it. Unfortunately, we could not use the fibre switch in the end due to high absorption, but now I can brag to my friends that I know how to weld. Also, special thanks to Anders Persson, thank you very much for letting us using your developed program, without your help, our setup will be hard to finish in time.

Sincere thanks to Lars Engström. You were my lecturer during the atomic physics course, and you helped me to find this thesis work. Thank you very much.

I would like to thank all my friends for the happy memories. I love the lunchtimes we spent together, and the snacks or stories you shared with me. Special thanks to Vidar Flodgren for staying up to fix my computer and helping me with Latex – you are a PC master. Also special thanks to Yupan Bao; I asked you so many questions related to thesis work and you never got tired of answering them. You helped me avoid so many mistakes.

Finally, I must express my very deepest gratitude to my parents and my boyfriend Karl Bastos. Thank you for your support and encouragement, not only through this thesis but with everything. Thank you so much, Karl, for every single night you stayed up with me. Thank you for cheering me up when I was down, and thank you for fulfilling every willful wish I had. You are the best.

Abbreviations

APD	Avalanche photodiode
UCNPs	Upconverting nanoparticles
UC	Upconversion
UCL	Upconversion luminescence
QY	Quantum yield
QD	Quantum dot
RE	Rare earth
BP	Bandpass
LP	Longpass
TPA	Two-photon absorption
ESA	Excited state absorption
GSA	Ground state absorption
ETU	Energy transfer upconversion
CUC	Cooperative upconversion
Yb	Ytterbium
Tm	Thulium
$NaREF_4$	Sodium Rare earth fluoride
$NaYF_4$	Sodium yttrium tetra fluoride
Tm^{3+}	Trivalent thulium ion
Yb^{3+}	Trivalent ytterbium ion
APD	Avalanche photodetector
ND	Neutral density
OD	Optical density
FWHM	Full width half maximum

Contents

Introduction 1

Optical molecular imaging is growing research discipline. It aims at developing good biomedical tools at levels ranging from subcellular structures to tissues. Its relative cost-efficient and very low toxicity makes it promising for both *in vivo* and *in vitro* applications. Molecular imaging has been widely applied in medical research, e.g., in understanding molecular mechanisms of cancer development and treatment. Fluorescence molecular imaging is an ideal tool for investigating biological samples [1] [2]. When a molecule absorbs a photon, an energetically excited state is formed. The excited electron from the molecule undergoes interactions with the host crystal lattice, the electron de-excites to its ground state, the excess energy from the molecule is released in the form of a photon. When the quantum energy precisely fits the energy gap between the up and down states, the transition happens. To enhance the quality of recordings, contrast agents (contrast media or dye), especially the exogenous types, are used in fluorescence imaging. The contrast agents can also be a pharmaceutical drug carrier. Common fluorescent contrast agents are quantum dots [4], organic dyes [5], and fluorescent proteins [6].

The next step to enhance the resolution of fluorescence imaging is to lower the background fluorescence. Background fluorescence provides a background and noise to the signal. It is thereby a detected signal that disturbs the measurement. The background fluorescence can be classified into two types: the background fluorescence from the experiment setup and the autofluorescence of the sample. Autofluorescence is the emission of light by an endogenous biological structure following absorption of light; it also happens in non-biological materials. Phenylalanie, tyrosine, and tryptophan inside proteins show some degree of autofluorescence [8]. The background noise caused by the instrument can be removed by modifying the setup, for example, the excitation wavelength can be filtered out by adding bandpass filters. The way to reduce the autofluorescence is a bit different; it helps to work in the optical window where the light absorption is low. The optical window corresponds to the red and near- infrared spectrum, where living tissue exhibits low absorption. An ideal biomarker should have its emission wavelengths in the region of the optical window, so the living tissue absorbs relatively little light, and the biomarker should be non-toxic and exhibit long luminescence lifetimes.

Lanthanide-doped upconverting nanoparticles (UCNPs) meet all the requirements to be a good biomarker. Upconversion contains sequential multiple photons absorption, where the upconverting nanoparticles are the combination of trivalent lanthanide ions with an appropriate inorganic host lattice, so that produce higher energy anti-Stokes luminescence. Especially the $NaYF_4$-based systems have been attracting extensive interest due to their unique optical proprieties for *in vitro* imaging application. Lanthanide ions are acting as sensitizer and activator [9]; they have long lifetime and a ladder-like energy levels structure. Rare earth elements include 15 lanthanides together with two additional elements, scandium and yttrium. The electronic configuration of lanthanides can be

described as $1s^2 2s^2 2p^6 3s^2 3p^6 3d^{10} 4s^2 4p^6\ 4d^{10} \mathbf{4f}^N 5s^2 5p^6 \mathbf{5d}^M 6s^2$, where N and M are integer numbers, specifying the number of 4f and 5d electrons for different elements. An activator is an ion doped into a lattice, emitting light following an excitation. A sensitizer is an ion in the crystal lattice that absorbs light and transfers the energy to the activator, often through a radiationless energy transfer process. The sensitizer-activator pair Yb^{3+}/Tm^{3+} is frequently used in fluorescence imaging research. The co-doped UCNPs can be excited by a laser light with a wavelength of about 980 nm and releases light at a wavelength of 800 nm; both wavelengths are very good for *in vivo* imaging.

The emission intensity of UCNPs shows a nonlinear dependence on the excitation power. An improved understanding and characterization of the UCNPs and their energy levels would potentially provide more information for improving the biomedical imaging applications. The UCNPs have the property of anti-Stokes shifting the emission with respect to the excitation light. When an emitted photon has more energy than the absorbed photon, their energy difference is called anti-Stokes shift. Anti-Stokes shift of the upconverted photoluminescence enables the detection of weak signals and allows a background-free imaging with a higher spatial resolution than with conventional fluorophores [3].

However, due to UCNPs' relatively low luminescent quantum yield, which is defined as the ratio between the amount of emitted and absorbed photons [10], the application of UCNPs is still somewhat restricted. The challenge of improving the efficiency of UCNPs' quantum yield has to be surmounted wisely. To date, researchers have shown there are multiple ways of enhancing the upconversion luminescence, such as polymer modification of $NaYF_4$: Yb^{3+},Tm^{3+} [11], upconverting nanocrystals doped with different concentrations of Li^+ions [12], and nanocrystals with resonant waveguide grating substrate [13]. To specifically enhance the intensity of 800 nm luminescence, there are methods such as increasing the content of Yb^{3+} ions [16], add Ho^{3+} ions as the second sensitizer [14] and specifically designing core/shell structures [17].

In this thesis, an upconverting nanoparticle quantum yield measurement system is developed. The concept is based on the experience from the previous master project by Björn Thomasson. The aim of this thesis work is to facilitate an enhancement of the upconversion luminescence of $NaYF_4$: Yb^{3+} , Tm^{3+} in fluorescence imaging by minimizing the influences from the surroundings and to simplify the measurement procedures. More specifically, the idea is to design a capable experimental setup of determining the quantum yield as a function of excitation power density. Such a system will facilitate the development of an improved quality luminescence particles imaging.

Theory 2

2.1 Quantum yield

As mentioned in the introduction chapter, the quantum yield (QY) is defined as the ratio between the amount of emitted photons and the amount of absorbed photons. It gives the probability of the excited stated being deactivated by fluorescence rather than by other non-radiative processes, i.e. the transition occurs without the emission of photons. The QY calculation formula is:

$$\eta \equiv \frac{N_{\text{em}}}{N_{\text{abs}}} = \frac{k_0 I_{\text{em}}}{I_{\text{ex}}}, \tag{2.1}$$

where N_{em} and N_{abs} represent the amount of emitted photons and the amount of absorbed photons, k_0 is a scaling factor which accounts for the photon energies at the two wavelengths involved, I_{em} represents the emission intensity and I_{ex} represents the excitation intensity. If there are n amount photons involved in the upconversion process, the QY is generally denoted by η_{norm} with the dimensions of $[\text{cm}^2\text{W}^{-1}]^{n-1}$:

$$\eta_{norm} \equiv \frac{I_{\text{em}}}{I_{\text{ex}}^n}. \tag{2.2}$$

2.1.1 Sample attenuation measurement

It is necessary to measure the excitation beam attenuation to calculate the amount of excitation photons absorbed by the sample. The attenuation could be due to the reflection at the solution interface and scattering inside the liquid, but mainly due to the absorption by the sample. When a laser light of initial intensity I_0 passes through the sample which was stored in the cuvette, some of the light is absorbed. Thus, the intensity of the transmitted light I_t is less than the initial I_0. The intensity loss can be measured with a blank cuvette filled with only the suspension liquid, and the light losses to the cuvette wall (the container) and the suspending liquid are negligible. The relation between I_0 and I_t are defined by the Beer-Lambert law:

$$A = log_{10}\frac{I_0}{I_t} = lc\epsilon, \tag{2.3}$$

where symbol A represents the measured absorbance, l represents the length of the light path [cm], c represents the concentration of solution [mol L^{-1}] and ϵ represents the molar absorptivity of the solvent [$\text{Lmol}^{-1}\text{cm}^{-1}$]. An ideal value for absorbance A is between 0.04 and 0.05 [7]. If absorbance is lower than 0.04, it will lead to error in the experiment, as there might be not enough fluorophore particle to emit detectable luminescence. On the

other hand, a relatively low absorbance ensures the emission intensity to be proportional to the particle concentration. By writing the wavelength dependent coefficient $\mu_t(\lambda)$ [m^{-1}] and light path l [cm], the transmitted light generally written as:

$$I_t = I_0 e^{-\mu_t(\lambda) l}. \tag{2.4}$$

Equation 2.4 is known for describing the transmitted light intensity after it passed through a medium. I_t [Wcm^{-1}] is the transmitted light intensity and I_0 [Wcm^{-1}] is the initial excitation light intensity, and both of them are wavelength dependent. The light intensity [Wm^{-2}] is defined as the power [W] transferred per area [m^2], the area is perpendicular to the direction of the power energy. Thus, equation 2.3 can be rewritten as:

$$A = log_{10} \frac{P_0}{P_t} = lc\epsilon. \tag{2.5}$$

In equation P_0 [W] and P_t [W] represent the power of the initial excitation power and the transmitted power.

2.1.2 The quantum yield determination by the comparative method

Experimentally, relative fluorescence quantum yield can be determined by using the Williams the comparative method [23]. Williams method involves a well-characterized sample with a known QY. In an ideal situation, both reference and test samples have the same experimental parameters (such as excitation wavelength, slit width, etc.); it simplifies the work to assume that both samples absorbed the same amount of photons. The QY is then calculated by:

$$\Phi = \Phi_{\mathrm{R}} \times \frac{Int}{Int_{\mathrm{R}}} \frac{1 - 10^{-A_{\mathrm{R}}}}{1 - 10^{-A}} \frac{n^2}{{n_{\mathrm{R}}}^2} \frac{q_R}{q} f, \tag{2.6}$$

where Φ represents the tested sample QY, Int is the integrated fluorescence intensity, q [$m^{-2}s^{-1}$] is the number of excitation photons per second integrated over the sample area, A is an absorbance at the excitation wavelength, f represents the filter factor (transmission rate) and n represents the solvent refractive index. The subscript R denotes the reference sample (with a known QY). The $\frac{q_R}{q}$ ratio is needed, to take into account the incoming photon flux for the absorption of the reference dye and the UCNPs sample, respectively. The number of photons at one wavelength can be calculated by dividing the excitation power in Watts [Js^{-1}] by the energy of the incoming photon [J], the ratio between the photon flux of the reference and the sample the equation simplifies to 785 nm / 975 nm, it is the value for $\frac{q_R}{q}$. However, in experiment there are numerous factors needed to consider, such as self-quenching (the decreases of the fluorescence intensity) due to a high concentration of solvent, different solvents may be used for reference and test sample or laser light scattering.

The considerations above can be solved by collecting data with a number of different concentrations and by carefully choosing the concentration range. DY-781-01 (Dyomics) is utilized as a reference sample in this thesis work. Ethanol was used as its solvent. Dye DY-781 exhibits a linear emission dependence on the excitation power density. DY-781 has its maximum absorption peak at 783 nm, and the emission peak at 800 nm [24]. A 20 μM DY-781 stock solution is diluted by mixing 5 μl of the stock solution with 4000 μl ethanol, due to the stock solution is too high concentration; its absorbance exceeds the limit empirical of 0.05 [7] where re-absorption starts to become an issue.

2.1.3 Filter factor

As shown in equation 2.6, the filter factor is one of the factors needed to correctly retrieve the QY value. To explain it, one example is provided in figure 2.1. The emission spectrum of DY-781 in ethanol was measured by previous master student Björn Thomasson [7]. All filters transmission raw data can be found on Thorlab; each filter transmission is plotted as a function of wavelength. The integrated fluorescence intensity of DY-781 without filter gives the value 57.8, while the integrated fluorescence intensity of the same dye when one 800 nm Bandpass (BP) filter is employed gives the value 19.3 and the integrated fluorescence intensity of the same dye when the 830 BP filter and Longpass (LP) filter are employed, the value is only 2.26. According to Björn's thesis, the DY-781 dye exhibits a QY of 11.9% when it is dissolved in ethanol. The use of equation 2.6 provides the expected QY values when one 800 nm BP filter used is 3.98%, and the QY when the 830 nm BP and LP filters both are utilized, is 0.47%.

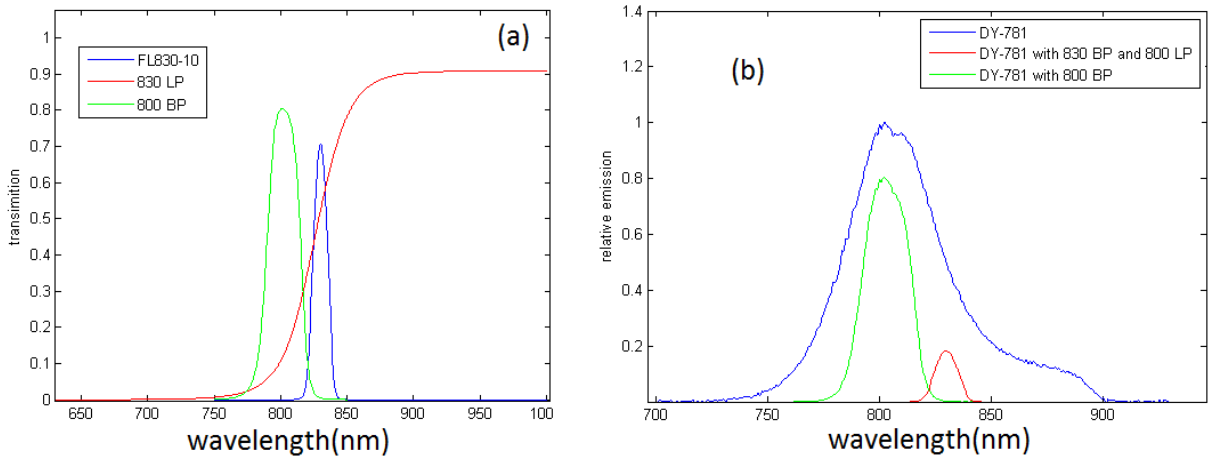

Figure 2.1: (a) The FL830-10 BP filter has maximum 70% transmission at wavelength 830 nm with a FWHM of 10±2 nm, the 800 nm BP filter has a maximum transmission of 80% with a FWHM of 20±2 nm. For the 830 nm LP filter, any wavelength shorter than 830 nm, is blocked. It has transmission 52% at wavelength 830 nm. (b) An example of how filters will affect the QY value. The blue plot line represents the dye DY-781 emission spectrum, green plot line represents the same dye emission spectrum, but with an 800 nm BP filter is in the emission detection path, the red plot line is when both the 830 nm BP and 830 nm LP filters are in the emission detection path.

2.1.4 The quantum yield coefficient

The quantum yield for UCNPs can be presented as a function of the excitation power density y [Wm^{-2}]. A factor a is defined as the maximum attainable QY of the system. It can be obtained by measuring the QY at very high excitation power; b [Wm^{-2}] is defined as the power density at the so-called balance point. The balance point is defined in a QY against power density plot, where a slope of 1.5 is considered the balance point [35].

$$\Phi = \frac{a \cdot y}{b + y}. \tag{2.7}$$

2.2 Upconversion mechanism

Upconversion is a family of non-linear optical processes that can be categorized as three basic mechanisms; excited state absorption, energy transfer upconversion and cooperative upconversion. Another well-known non-linear optical process is two-photon absorption (TPA), which requires simultaneously absorption of two photons to induce a transition to the excited state. Unlike TPA, upconversion does not require simultaneous absorption of photons. Upconversion process is instead a sequential absorption of several photons. The frequently light will excite the ion to long-lived metastable energy state allowing sequential absorption events. One of the significant features of upconversion is the anti-Stokes shift of the luminescence emission. This feature allows upconversion luminescence (UCL) materials to emit shorter wavelength than the exciting light.

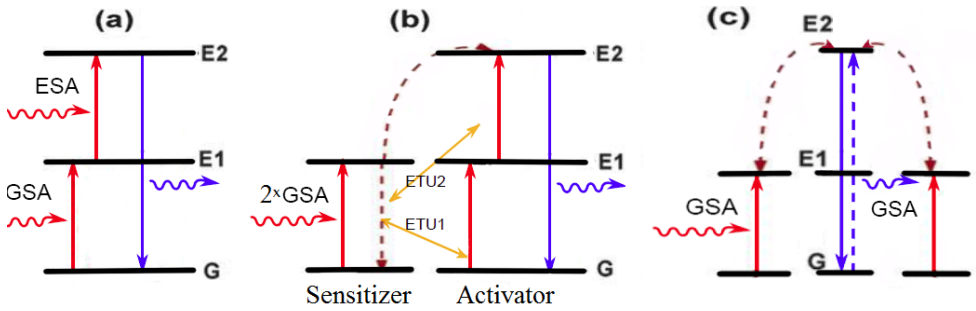

Figure 2.2: Principal upconversion processes for UCNPs. (a) Schematic diagram of excited state absorption (ESA) following a ground state absorption event (GSA). (b) Schematic diagram of the energy transfer upconversion (ETU) following GSA. (c) Schematic diagram of cooperative upconversion (CUC).

2.2.1 Excited state absorption

Excited state absorption (ESA) occurs only when the RE ion already has been excited by ground state absorption (GSA). The GSA process is when an ion is photo-excited from the ground state **G** to the metastable state **E1**. In the case, the RE ion absorbs additional pump photons to excite the ion from the metastable state **E1** to higher excited state **E2**. This process is called ESA. The ESA and GSA transitions are illustrated in figure 2.2(a). Upconversion emission is generated when ions in the **E2** state are de-excited to the ground state **G** and release the excess energy in the form of one photon per de-excited ion.

2.2.2 Energy transfer upconversion

As mentioned above, ESA happens for a single ion. When there are two neighboring ions involved, the non-radiative energy transition happening between them is called energy transfer upconversion (ETU). This process involves two ions: a sensitizer ion and an activator ion, as illustrated in figure 2.2. The energy transfer upconversion between two neighboring ions is considered as a non-radiative process, the transitions without the emission of photons, and the excess energy is dissipated in the form of photons and associating with lattice vibrations. Two non-radiative energy transition can happen, between excited and ground state (ETU1 in figure 2.2(b)) or between two excited states (ETU2 in figure 2.2(b)). The latter transfers the activator ion from the metastable state to a higher

excited energy level **E2**, while the sensitizer ion returns to electric ground state **G**. The concentration of dopant is very critical; it determines the distance between neighboring ions which affects the energy transfer between two ions and the upconversion rate. The probability for energy transfer is defined as:

$$P_{SA} = \frac{(R_0/R)^n}{\tau_s}, \tag{2.8}$$

where τ_s [s] represents the sensitizer lifetime, R_0 [m] is the transfer distance for which excitation transfer and spontaneous deactivation of sensitizer have equal probability, R [m] is the distance between two dopant ions. The number n is a positive integer which has different value for different interaction [18] :

- n=6 dipole-dipole interactions
- n=8 dipole-quadrupole interaction
- n=10 quadrupole-quadrupole interaction

The ETU process has been seen in numerous types of ion doped crystals. The one issue with ETU is the non-radiative decay that leads to unwanted heat in the crystal. However, due to it allows efficient energy transfer from sensitizer to the activator, it is still wildly used in creating new upconversion nanomaterial.

2.2.3 Cooperative upconversion

Cooperative upconversion (CUC) is the interaction between three ions as illustrated in figure 2.2(c). At least two adjacent sensitizers simultaneously provide energy to the activator, the combined energy excites the activator ion to the higher excited state **E2**. Following this process, the ion returns to its ground electronic state and releases upconversion luminescence. This progress is called cooperative luminescence. CUC happens in Yb^{3+} singly doped crystal as a cooperative luminescence [30] and acts as a cooperative sensitization in bulk material Yb^{3+}/Tb^{3+} or Yb^{3+}/Eu^{3+} [31].

2.3 Upconverting nanoparticles

Lanthanide-doped upconverting nanoparticles, especially the $NaYF_4$-based systems, hold promise as novel luminescent probes for numerous applications in biophotonics. In general, UCNPs are formed by doping inorganic host crystal with rare-earth (RE) ions. The presence of RE ions the crystal may provide luminescent, while some inorganic crystals may not show upconversion (UC) luminescence by themselves. UCNPs are anti-Stokes shifting [9] the upconverted photoluminescence signal. This property enables a background-free imaging, and also with an improved spatial resolution, allows to detect weak signals in the presence of tissue autofluorescence. In this thesis sodium yttrium fluoride crystals have been employed doped with trivalent ytterbium ions and trivalent thulium ions ($NaYF_4$: Yb^{3+}, Tm^{3+}). $NaYF_4$ is among the most efficient host material for upconverting luminescence, and Yb^{3+}/Tm^{3+} activator-sensitizer pair is frequently used in recent research.

2.3.1 Activator and sensitizer

The way activator ion works is by letting the ion undergo a series excitation process to reach a high-lying bound state. When the excited electron returns to its ground state it releases energy in the form of a photon, an upconversion luminescent is achieved. A good activator has multiple long-lived metastable energy levels that match the excited energy levels of the sensitizer. The activator luminescence wavelength range shall fulfill the application demand: in this thesis, it is around 800 nm. A good sensitizer should have a simple energy structure and relatively long-lived excited energy levels. The excited sensitizer ion transfers energy multiple times to the activator ion to indirectly excite this ion. The schematic energy level diagram of the sensitizer and activator used are shown in figure 2.3.

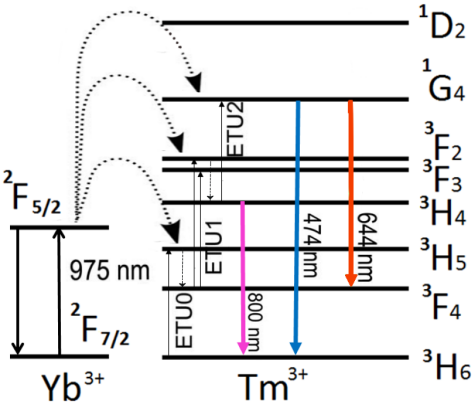

Figure 2.3: Schematic energy level diagrams of the sensitizer ion Yb^{3+} and activator ion Tm^{3+}. The proposed upconversion mechanism with the following excitation at 975 nm and emission at 800 nm.

Activator and sensitizer ions are chosen from Lanthanide elements. Trivalent erbium and trivalent thulium ions are amongF the most utilized activator ions, and trivalent ytterbium ion is one of the most utilized sensitizers in UCNPs. Lanthanide elements are characterized by their partially filled 4f shells which allow the electron transition between 4f and 4d levels. Sensitizer harvests energy and transfers to activator ions. Tm^{3+} ion as an activator, fulfills the requirements, and it has relatively large energy gaps to reduce the nonradiative transfer (the sensitizer separated energy level is being resonant with the corresponding energy gap in activator). Yb^{3+} ion as a sensitizer, its ground state is $^2F_{7/2}$ and it one excited 4f state $^2F_{5/2}$. Its simple structure nicely fits the energy structure of activator Tm^{3+}.

2.3.2 Host material

The primary requirement for the host material is that it should have a good lattice matching with the dopant ions; the distance between dopant ions, relative spatial position, and coordination numbers [21]. Upconversion relies on energy transfer between activator and sensitizer within a close range. A suitable host material needs to be able to host the activator and sensitizer ions within a proper distance to allow generating strong luminescence.

Secondly, low phonon cutoff energy and low crystal field symmetry are preferred; they can decrease non-radiative loss during upconversion and increase the emission. The

luminescence intensity is sensitive to the distribution of phonon density; the non-radiative process is the main loss for upconversion emission [22].

Fluoride based crystals, oxide based crystals and many other different materials are used to as crystal host material in UCNPs. $NaYF_4$ seems today to be the most promising material for UCNPs, and there are two different type of it, cubic (α) $NaYF_4$ and hexagonal (β) $NaYF_4$, see figure 2.4. The $NaYF_4$ phase can be transformed in $NaREF_4$ structures by lanthanide doping [19]. For example by adjusting the Y^{3+}/F^- ratio in the synthesis reaction solution one can change the $NaYF_4$ phase between cubic and hexagonal. The host material phase affects the upconversion emission; efficiency low phase symmetry contains more uneven components which allow a stronger coupling between 4f energy levels and give higher upconversion emission efficiency.

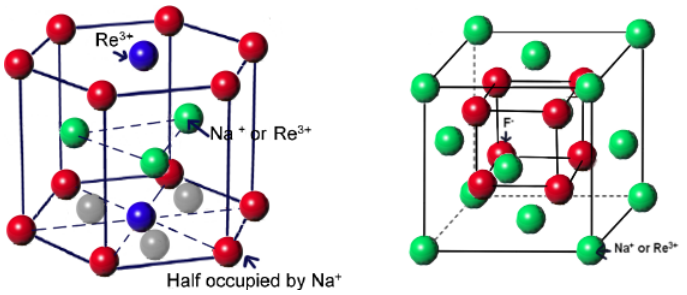

Figure 2.4: Structure of a hexagonal and cubic phase of $NaYF_4$ crystal. The figure on the left-hand side is the hexagonal structure, green color balls represent the Na or RE atoms and their projection on the bottom lane are shown by gray balls, the red color balls represent the half empty half occupied Na atom, and the blue balls represent the RE atoms. The figure on the right-hand side is the cubic structure, where green balls represent the Na or RE atoms, and red balls are F atoms.

In cubic $NaYF_4$, $Y^{3+}$and Na^+ ions are randomly distributed on the host material cation sites, but in hexagonal $NaYF_4$, there are three cation sites only and one for Y^{3+} ions, one for Na^+ ions and the last one for both Y^{3+} and Na^+ ions [15]. Hexagonal-$NaYF_4$-based UCNPs have been proven to be the most efficient [20], it is a much better host lattice for the luminescence of RE ions than the cubic $NaYF_4$.

2.4 Luminescence anisotropy

Light is a harmonic electromagnetic wave. When it interacts with an object, usually its magnetic effect can be neglected. Natural light or fluorescence contains all possible orientations of the electric field vector directions. When the direction of the electric vector does not change during propagation, it is called linearly polarized. When the random light goes into the polarizer, only the light polarized in the given direction can pass through the polarizer. Polarization is a fundamental property of light [32].

The fluorescence from the sample is the combination of signals from individual fluorophore dipole emissions; it is the key to how the polarization and fluorescence are connected. An electric dipole is defined as the separation of positive and negative charges. The dipole moment represents the strength and direction of the dipole. The possibility of a transition of a molecule between two energy states is proportional to $cos^2\phi$, where ϕ is the angle between the direction of excitation polarized light and the dipole moment. Thus, when the excitation light is parallel to a molecule's dipole moment, the molecule

has the highest chance to absorb a photon. On the other way around, if the polarized excitation light is perpendicular to the dipole moment, the molecule cannot be excited. The degree of polarization can be obtain by studying the polarization ratio (p) and emission anisotropy (r);

$$p = \frac{I_{\parallel} - I_{\perp}}{I_{\parallel} + I_{\perp}}, \tag{2.9}$$

$$r = \frac{I_{\parallel} - I_{\perp}}{I_T} = \frac{I_{\parallel} - I_{\perp}}{I_{\parallel} + 2I_{\perp}}, \tag{2.10}$$

where $I_{\parallel}$ [Wm^{-2}], is the intensity measurements made parallel to the emission light, and $I_{\perp}$ [Wm^{-2}] is the intensity measurement made orthogonal to the emission light. Both measurements can also be made by rotating the polarizer in the excitation path instead of emission path. The direction of emission dipole affects the value and sign for p. When the dipole moment and the electric field are parallel to each other p equals 1, and when the dipole moment is perpendicular to the electric field, p equals -1. Emission anisotropy (r) is preferred as it contains the total intensity I_T. The reason I_T equals $I_{\parallel} + 2I_{\perp}$ is that

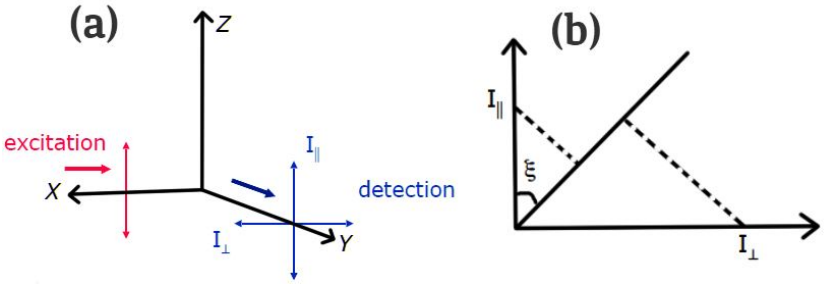

Figure 2.5: (a) An illustration of fluorescence polarization measurement. The incoming light in excitation path is linearly polarized, and the resulting fluorescence composed of the combination of measurements $I_{\parallel}$ and $I_{\perp}$. (b) An illustration diagram of a polarizer oriented with an angle ξ, and how it is related to both $I_{\parallel}$ and $I_{\perp}$ in the emission path

in geometry only light of one polarization is detected, while light polarized both in the x and y-direction will have the same intensity $I_{\perp}$. If there is no polarizer in the emission path, the detector measures the $I_{\parallel} + I_{\perp}$, which does not equal the total intensity. To get a value for the total intensity, it can either measure separately $I_{\parallel}$ and $I_{\perp}$ and calculate I_T or place a linear polarizer in the emission path with a given magic angle, 54.74°. To calculate the magic angle, an analysis diagram is presented in figure 2.5. Assume at an angle ξ which can obtain $I_{\perp}$ with double weight than $I_{\parallel}$:

$$I(\xi) = I_{\parallel} cos^2\xi + I_{\perp} sin^2\xi, \tag{2.11}$$

$$sin^2\xi = 2cos^2\xi, \tag{2.12}$$

$$tan^2\xi = 2, \tag{2.13}$$

$$\xi = 54.74°. \tag{2.14}$$

Experiment 3

3.1 Experiment setup

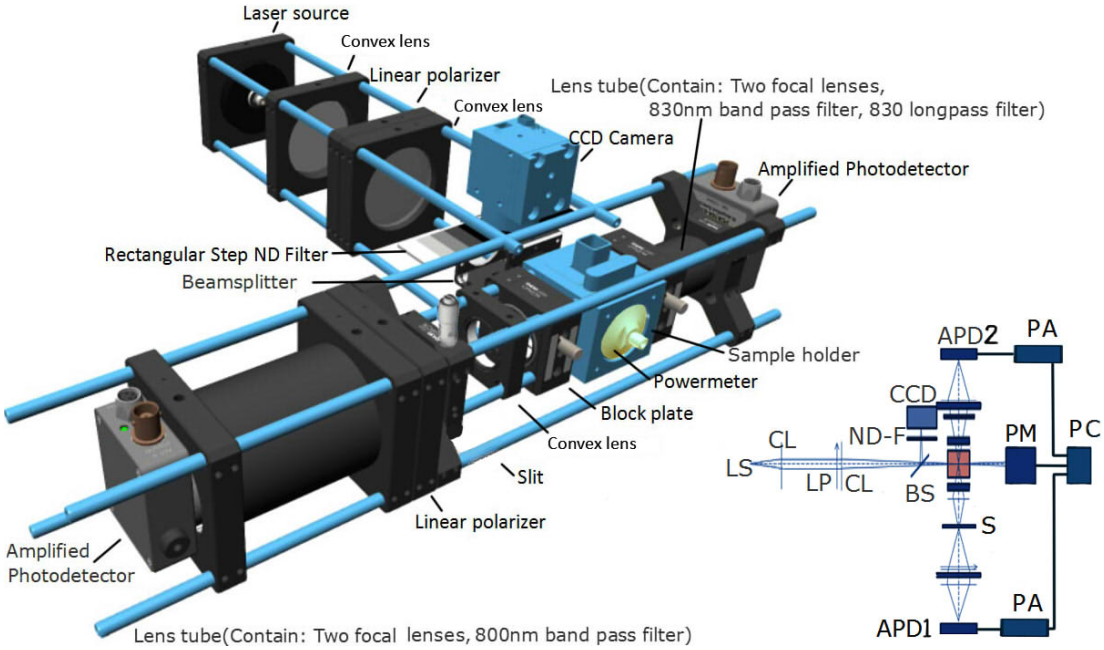

Figure 3.1: An illustration of the relative quantum yield measurement system. A simpler illustration diagram is inserted at the bottom right corner. All components are mounted along a common optical axis; it simplifies the beam alignment process, the entire setup in this way can easily be transported. The distance between APD1 and APD2 is about 42 cm, the distance between the laser source and power meter is about 35 cm, so the size of the system is relatively small. Both APDs are connected to a preamplifier to boost the signal strength with two different input channels.

In this chapter, the developed system is presented. The setup and a block diagram can be seen in figure 3.1. The design of the setup is based on the filter fluorimeter concept to characterize the luminescence of quantum yield. The important optical components usage is explained in the following sections. The entire setup is covered with black cardboard to block the surrounding background light; a cap made of black paper is used to cover the top of the sample holder. Three optical fibers were used in the setup; two optical fibers were used to connect the laser drives to a simple fiber switch. For the third optical fiber, one side of it is mounted to the setup and the another side is momentarily mounted to the fiber switch depends on which wavelength is going to be used.

3.1.1 Fluorometer

A filter fluorometer can be built at a low cost. It is easy to modify, but it is not the ideal choice since it can only look at a fraction of the emitted photons. The coherent light beam emitted by the laser system (excitation source) will be expanded after it passes through an excitation lens. This process is important for the beam profile measurement with the profiler. It is not required for normal dyes but only for UC materials, since they are dependent on the excitation power density. After passing through the excitation polarizer, the laser beam is separated into two beams; one is detected, and the other beam passes through the sample. The avalanche detector (APD) is located a distance away and at a 90-degree angle from the sample. It is used to detect fluorescence. The BP and LP filters are used to select the wavelength, while the BP filter blocks unwanted radiation and transmits a well-defined wavelength band of light. The LP filter blocks wavelengths shorter than the defined cut-on wavelength to minimize the potential leakage from the laser to disturb the measurement.

3.1.2 Light source

For the UCNPs and the reference dye DY-781 corresponding excitation wavelength are 975 nm and 785 nm separately. Two diodes from Thorlabs were used to provide these wavelengths, label L975P1WJ and L785P090. The maximum current one can apply to the L975P1WJ laser diode is 1.8 A, and the maximum current one can use for L785P090 diode is 160 mA. The maximum radiation power obtained by the power meter is 200 mW for the 975 nm diode and 20mW for the 785 nm diode. The laser beam loses power in the optical fiber, linear polarizer, focal lens and beam splitter. The optical fiber used during the measurement has a core size of 600 μm.

3.1.3 The excitation path

The excitation path is defined as the beam path from the laser source (fiber adapter) to the sample holder. A multimode optical fiber transfers the laser light from the laser diode mount to the system. The fiber end is connected to the laser source fiber adapter, the fiber adapter is adjusted by two small screws to move the laser beam spatial position vertically and horizontally. The laser mount is connected to both a laser diode current controller and a temperature controller. The temperature for the laser driver is always set to a constant value of 25 °C. A distance of 7 cm away from the adapter there is a 60 mm cage plate mounted with a convex lens (f=9 cm). It expands the laser light. Those 60 mm cage plates used in the setup are designed to hold Ø2"(diameter 50.8 mm) optical components with various thicknesses. Another convex lens (f=22 cm) is mounted 7.5 cm away from the first convex lens. Besides a linear polarizer was placed here to ensure that the laser light interacting with the sample is linearly polarized. A magic angle detection in the right polarized is needed for this measurement. This is discussed more details in section 2.4. Then 12 cm away from the second convex lens is the beam splitter. It separates the beam into two directions with an intensity ratio 8:92. The 8% light passes through one rectangular ND filter and reaches a CCD camera, the 92% light is directed through the sample. It is very important that the distance from the center of the beam splitter to the CCD camera and the center of the sample is the same; 6.5 cm in this case. The CCD camera is used to analyze the beam cross section profile. The rectangular step ND filter is interchangeable, and it has ten different optical densities, from OD 0.1 to 4.0.

3.1.4 The emission path

The emission path is directed at a 90-degree to the excitation path. It is the range between the two APDs in figure 3.1. The sample is contained inside a UV fused quartz cuvette with four polished sides; this allows optical access from the four sides used. The power meter is mounted to the right side of the sample holder, and the sensor side is facing the excitation path direction. The power meter is used to examine the laser beam and record laser power before and after the sample is placed. The concept with data collected both by the power meter and the CCD camera enables to obtain the power density at the sample. The laser beam profile is examined by the CCD camera. Since both current and temperature can alter the beam profile, it is necessary to examine the beam profile during the measurement.

So for both the top and bottom sides of the sample holder, there is a mechanical shatter placed next to it. It is used to protect the APD from high-power beam damage. Along the direction where APD1 locates, 5 cm away from the sample holder a convex lens is placed to collect the emitted luminescence. A slit with a width of 1.0 mm is placed 5 cm away from the convex lens to block the out of focus light. As the detection is dependent on the laser power, the placement of the slit is to select only the center of the beam for the detection, to ensure the same excitation power throughout the detection path. At a distance of 6 cm away from the slit, a linear polarizer is placed. It is rotated 54.74 ° compared to the polarization direction of the reference polarizer (the first polarizer in the excitation path). The polarized light will pass through two convex lenses and one 800 nm BP filter in a lens tube. The filtered light reaches the APD1 in the end. Along the direction where APD2 locates, the luminescence light passes through one 830 nm BP filter and 830 LP filter. DY-781 has a very broad emission, and it is possible to excite it at short wavelengths. The 785 nm laser was already available in the lab, so it was used to excite the DY-781 dye. The wavelength 785 nm is very close to the emission wavelength; an LP filter is needed to cut off unwanted radiations. The filtered light passes through two convex lenses and reaches APD2. Both detected signals will be fed to a preamplifier with a 20x gain. The reason chose 20 is because that is the highest factor it can boost the signal strength before the preamplifier is overloaded. The preamplifier is employed to reduce the interference and noise in the recorded signal. The prepared signal will be sent to a computer for further data analysis.

3.1.5 The excitation power detection

As mentioned in section 3.1.3, a power meter is placed in line with excitation path; it is ideal for metering low power light sources. The power meter is also named photodiode power sensor. The incoming laser power causes the photodiode sensor to deliver a corresponding current to a trans-impedance amplifier, which will be converted to a proportional voltage value. The power meter used in this system is Thorlabs PM16-121 standard photodiode power sensor with wavelength range 400 - 1100 nm. The maximum power range is 500 mW [25]. The power meter can be controlled by the Thorlab's power meter software PM100. The wavelength should be set individually with an actual wavelength value, as the power meter response is wavelength dependent. The software calculates the optical power from the measured current; it presents a time scale plot for each measurement; the data can be saved as a text file. To get power density value, the beam cross section measurement is required. A CCD camera is used to characterize the incoming beam and to help align the system. The CCD camera used in the thesis is a Thorlabs DCU224M

CCD camera with 1280x1024 pixels resolution [26]. The advantage of a CCD camera is its high dynamic range, i.e. it is capable of a wide range of intensities of light and it also has low noise which is ideal for low power source imaging. The software used to obtain the image from the camera is developed by Anders Persson, Atomic Physics, Lund University. The name of the software is 'LabView Laser Beam Profiler - Stabilizer'. The program is written in LabVIEW. The acquisition panel is mostly used; it selects a region of interest, subtracts a recorded background and saves the image to the computer. Calculated panel from beam profiler program can control and display the fit to a Gaussian beam profile, and the ideal beam type is top-hat. Thus, the CCD camera is also used to examine the beam type. An extra program Fiji [27] is used to analyze the raw image saved by the beam profiler program and calculates the beam cross section size where each pixel size is 4.65 μm x 4.65 μm.

3.1.6 Luminescence detection

The emission detection path with the 800 nm BP filter is the most important one, as it can be used for both UCNPs and DY-781 fluorescence measurements. The APDs used in this thesis is Thorlabs APD410A/M, which has a detection wavelength from range 400 to 1000 nm. It is furthermore temperature compensated [28]. This APD has low noise and high sensitivity. It is ideal for low optical power measurement. The software SIGAV LabView 2015 is used to read the output from the APD and save the data as a text file. This program is also developed by Anders Persson, Atomic Physics, Lund University. The emission detection path with the 830 nm BP and 830 nm LP filters, does not contain a linear polarizer. The reason of having this side is to allow the system to perform other dye measurements rather than UCNPs and DY-781 only. An issue with the 800 nm side in the arrangement is that all optical components are very packed. The 800 nm BP filter is mounted inside a lens tube. To change the filter, the system needs to be dismounted, and after changing the filter, the lenses needs to be re-calibrated. Both the DY-781 and UCNPs used have a strong emission peak around 800 nm, meaning that the signal can be detected with the 800 nm detection path. If other reference dyes are used, like Pacific Orange, which has an emission peak at 500 nm, it will not be detectable with the 800 nm detection side. The 830 nm BP and LP filters can be easily exchanged. It enables the measurement for different reference dyes. The problem with this side is that the detected emission signal is dependent of a possible emission anisotropy, as the emission intensity is not the total intensity.

3.2 Measurement procedures

Laser safety goggles must be worn during the measurement. The goggles should block the used wavelength range. The UCNPs sample solution and stock DY-781 solution were all a prepared by previous Biophotonics group member, Haichun Liu. The DY-781 stock solution of 20 μM was diluted by mixing 5 μl stock solution with 4000 μl of ethanol to minimize any re-absorption within the cuvette. The absorbance shall not be higher than 0.05 [7]. For the UCNPs, the molar ratio between Y^{+3}, Yb^{+3}, Tm^{+3} ions is about 75:24.7:0.3, the details of the UCNPs synthesis can be found in Xu et al. article [29]. The measurement procedure is divided into two parts; procedure 3.2.1 for the reference dye DY-781 measurement and procedure 3.2.2 is for UCNPs measurement.

3.2.1 Reference dye measurement (Timing ∼ 60 min)

Two cuvettes (10 mm × 10 mm) were cleaned and dried out. Water and ethanol were used to clean the cuvettes. One cuvette was filled with a 2mL diluted DY-781 solution; this cuvette is called the sample cuvette, and the another cuvette was filled with 2mL ethanol; this cuvette is called the blank cuvette. The ethanol used was F-sprit 95% (Contains 95% denatured alcohol). The absorption spectrum of DY-781 was provided by the product company [24], and the emission spectrum was measured by the previous master student Björn.

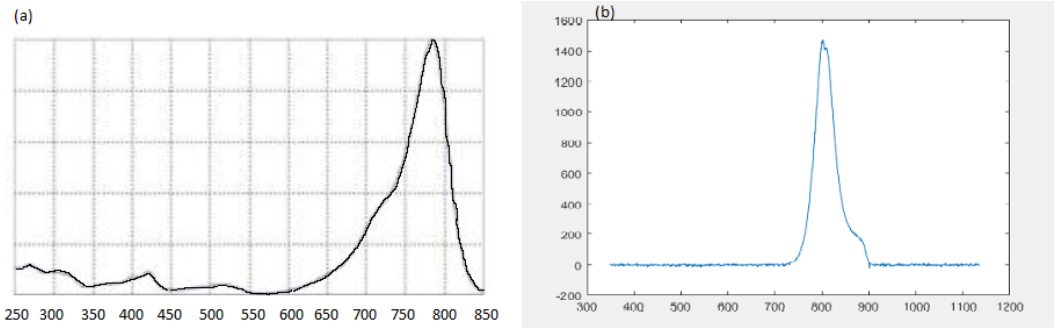

Figure 3.2: (a) The absorption spectrum provided by the producing company. For DY-781 has the maximum absorption peak is at 783 nm. (b) The emission spectrum of DY-781 in ethanol. The dye has maximum spectrum emission peak at 800 nm, and the second peak at 830 nm.

The laser with the excitation wavelength 785 nm was chosen to excite dye DY-781; the wavelength 785 nm is close to the maximum absorption peak of the reference dye. For both the power meter and the APD read out programs, integration time was set to 1.0 s and the total measurement time was 200 s. The APD has a sample rate of 25000.00 Hz, that means in each one second the program takes the average value out of 25000 detected signals. The temperature controller was turned on and set to 25 °C, then laser driver was turned on. The blank cuvette was placed inside the sample holder. The laser current was adjusted to the first measure data point. Both APD and power meter programs were started at the same time. After simultaneously recording for 60 s, the blank cuvette was removed to record the background for another 65 s. After that then the sample cuvette was placed in the holder and recording continuously till both programs stop after 200 s.

During the data evaluation, the data region of 5-55 were used for blank sample evaluation, data points 70-120 were used for the empty holder and data points 140-190 were used for sample evaluation. The procedures were repeated for multiple data points till reaching the laser driver limit power. In the continued measurements, the data points follow the power densities with a step size $10^{0.15}$ mWcm^{-2} while the first data point was $10^{0.6}$ mWcm^{-2} (the beam area were assumed to be 0.005 cm^2). In the reference dye measurement, a second APD (name APD2) were used. Unlike the first APD, APD2 its emission detection path does not have a slit and a linear polarizer. Instead, it has one 830 nm BP filter and an 830 nm LP filter and two focal lenses. The measurement procedure was the same as when using APD1.

3.2.2 UCNPs measurement (Timing ∼ 90 min)

For the UCNPs with Tm^{3+}/Yb^{3+} sensitizer and activator pair, exhibit emission spectrum showing strong emission in the NIR, red and blue following excitation at 980 nm. Thus, a laser with excitation wavelength 975 nm was chosen. The UCNPs measurement procedures were very similar to the reference dye measurement.

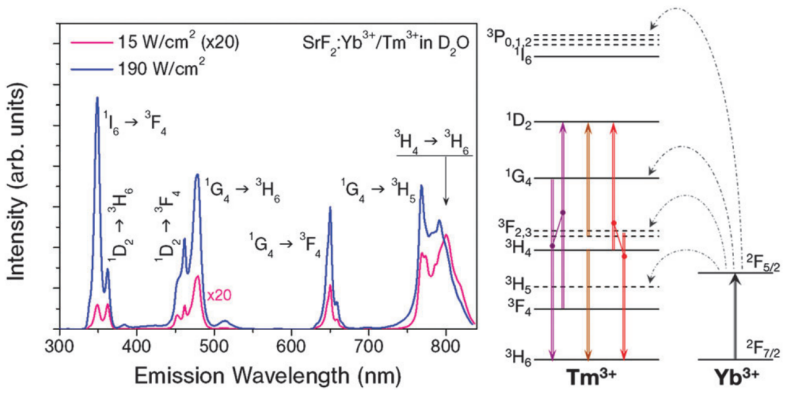

Figure 3.3: On the left-hand side is the emission spectra of SrF_2: Tm^{3+}, Yb^{3+} at room temperature. The picture on the right-hand side was Tm^{3+}/Yb^{3+} sensitizer and activator pair energy diagram. The figure was cited from Journal of Materials Chemistry C, 2015.3.3108 [33] without any modification.

Two cuvettes were cleaned and completely dried. It is important to know if the cuvette stored fluorophores before. Hydrogen chloride was used to remove the possible UCNPs inside the cuvette wall; the cuvette was filled with hydrogen chloride for at least one hour. Afterward, the hydrogen chloride was poured out, and the cuvette was cleaned with water and ethanol. One cuvette was filled with 2 mL cyclohexane, and another cuvette was filled with 2 mL of the UCNPs dispersion. The UCNPs emission spectrum is in figure 3.3 when it is under 980 nm wavelength excitation. The detection side with 800 nm BP filter was used. Both the APD1 and power meter readout programs; their measurement time was 200 s and the integration time was set to 1.0 s. The APD has a sample rate 25000.00 Hz. The temperature controller was always set to 25 °C, the laser driver was turned on. The cyclohexane blank sample was placed in the sample holder. Both the APD and power meter readout programs were started the same time. After measured for 60 s, the cyclohexane cuvette was removed to record the background for another 65 s, then the UCNPs sample cuvette was placed, and recording kept until both programs stop. After one measurement is performed, the laser driver current was set to a low value (where the beam was not saturated and can clearly see the beam shape); then a beam profiler picture was recorded. During data evaluation, the data region of 5-55 was used for blank sample evaluation, data points 70-120 was used for the empty holder and data points 140-190 was used for sample evaluation. The procedures were repeated for multiple data points till reached the maximum laser power. The data points follow the power densities with step size $10^{0.15}$ while the first data point was $10^{1.75}$ $mWcm^{-2}$ (The beam area was assumed to be 0.5 mm^2).

Results & discussion 4

This chapter will present the obtained result and analysis the data. Start with measured DY-781 power meter data. In figure 4.1(a), it can be seen from the trend of each measurement that the 785 nm laser is not very stable at a relatively high power. The variation of laser power would affect the fluorophore luminescence signal, which can be seen in figure 4.1(b), the luminescence varies along the time, especially the measurement represented by the purple line. Each color line in luminescence plot corresponds to the same color line power meter measurement, different colors represent a different group of measurements. In the luminescence plot, the scattering light was detected by APD (the measurement of empty sample holder increases when excitation power increases). This is due to the spectral range of blocked light of the 800 nm bandpass is too wide, allowing the scattered excitation wavelength 785 nm to be detected.

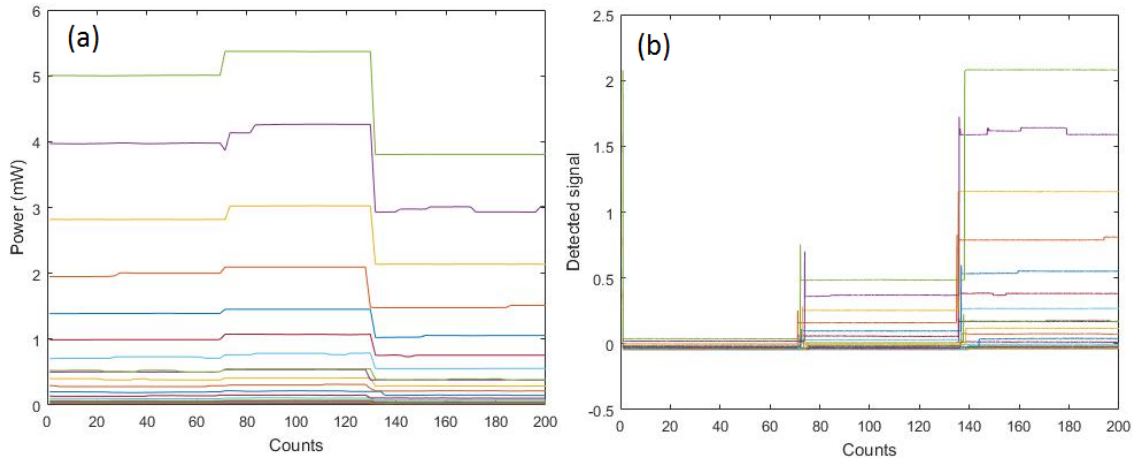

Figure 4.1: The recorded power meter measurement(a) and the recorded luminescence signal(b) for ethanol, empty holder, and reference dye DY-781. The counts between 0 to 60 are the measurement of ethanol, the region 60 to 135 is for an empty sample holder and the region 135 to 200 is when the reference dye is placed.

In UCNPs power meter measurement, compare figure 4.2(a) to figure 4.1(a), the 975 nm laser is more stable when it is at a high power region, it has very low variation. Thus, the luminescence signal detected will be relatively stable as well, which can be seen in figure 4.2(b). In the luminescence plot, the region between 0 to 60 is for cyclohexane, as can be seen in the figure it is grounded. The region 60 to 135 is when the sample holder is empty; the signal is grounded, which means the APD does not detect any scattering light. The 800 nm BP filter suppresses the excitation light sufficiently to block the scattered wavelength 975 nm. The region 135 to 200 is when the UCNPs sample is placed. The

curves show the signal responses of the UCNPs when the excitation laser power increases.

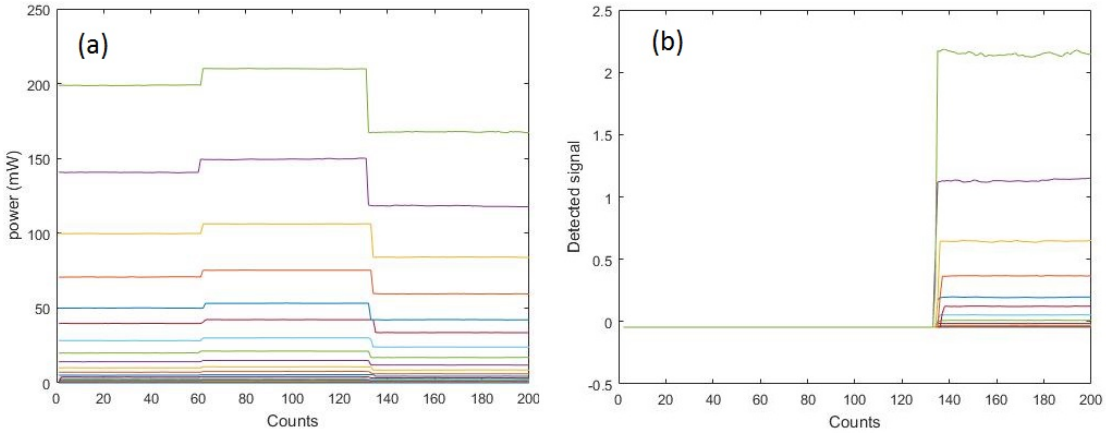

Figure 4.2: The recorded power meter measurement(a) and the recorded luminescence signal (b) for cyclohexane, empty sample holder and UCNPs. The region 0 to 60 is the measurement of cyclohexane, the region 60 to 135 is for an empty sample holder and the region 135 to 200 is for UCNPs.

The Dye DY-781 exhibits an 11.9% QY when it is dissolved in spectroscopic grade ethanol [7]. An expected QY value for DY-781 at the emission wavelength 800 nm is 3.98% (within the narrow filter used), and at the wavelength 830 nm, it gives a QY 0.47%. Both two expected QY values were examined by Marco Kraft [34] by comparing the data collected with his standard dye IR140 and reference dye DY-781 using the system built in this thesis with emission wavelength 800 nm. Marco measured the QY for dye DY-781 at 800 nm to be 4.49% and the QY at 830 nm to be 0.39%, while he made an absolute determination of the QY of IR140 in Berlin beforehand. Thus, the stock DY-781 dye is still available to use, and the expected QY values are reasonable. The detected signal for reference dye DY-781 is plotted against laser power density in a double logarithmic scale, see figure 4.3; both slopes values are close to the theoretical value 1.

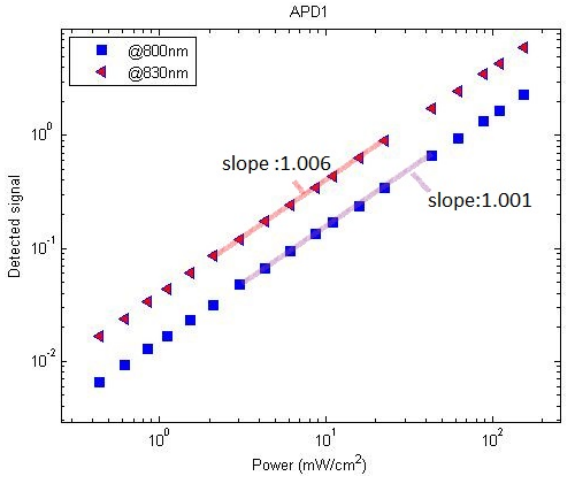

Figure 4.3: Detected DY-781 luminescence signal plot against laser power density in double-logarithmic scale. The red triangles represent the measurement at 830 nm wavelength while the blue square dots represents the measurement at 800 nm.

The reference dye is linearly dependent on the excitation power density. The magnitude ratio between wavelength 830 nm and 800 nm is 2.36. For 830 nm, its ethanol and luminescence signal plots are very similar as figure 4.1(b), but with a magnitude 2.36, thus it is not included in the result part.

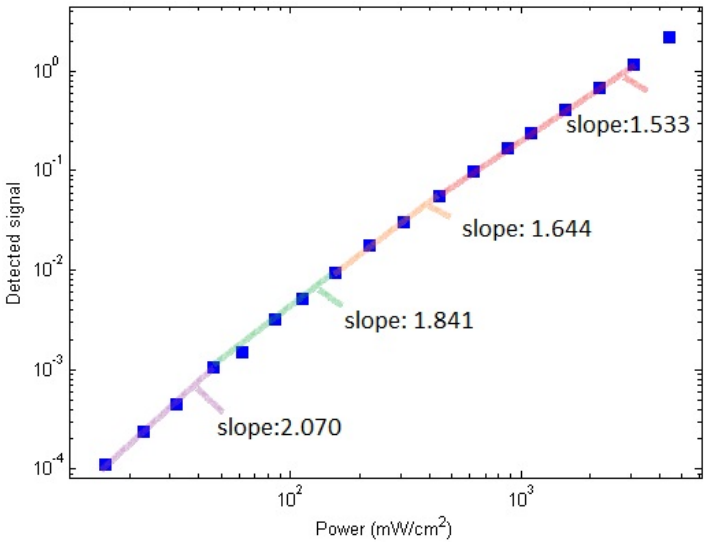

Figure 4.4: The power density dependence of core UCNPs upconversion emission at 800 nm in a double-logarithmic scale. The measured beam area is 0.05 cm^2.

For UCNPs, theoretically, the slope starts at value 2 and decreases to value 1 at high power density. Unfortunately, the 975 nm laser driver used during this thesis cannot reach excitation power higher than 200 nW. However, the data collected still provide enough information to prove the upconversion emission is nonlinear dependent on the excitation power density, see figure 4.4.

In section 2.1.4, it was mentioned that the balance saturation point is when the upconversion emission power density dependent plot has a slope of 1.5. To present the QY as a function of the excitation power density, the experimental data can be fitted with equation 2.7. The a value is defined as the maximum attainable QY, since setup limitation this value cannot be obtained experimentally. The a value is instead estimated to be twice the QY at the balance point [35], equaling 0.23%. The b value is defined as the power density at the balance point. It equals 2250 mWcm^{-2}.

Back to the UCNPs upconversion mechanism, its emission intensity is non-linearly dependent on the excitation power density, the measured beam area is 0.05 cm^2, see figure 4.4. As shown in equation 2.2, the n-power is directly related to the slope of the double-logarithmic plot, see figure 4.4. UCNPs upconversion emission is quenched due to relevant non-radiative relaxation processes [33]. If the relaxation has a higher probability to occur than the upconversion, the slope of the curve will equal to n. However, since UCNPs is in a crystalline lattice host, with relatively low phonon energies, upconversion has a higher possibility to occur than relaxation. Saturation happens with increasing of excitation power density; the slope value becomes lower than n for the same upconversion emission band. Energy levels are saturating and therefore less low energy photons are required to produce one high energy photon. The QY will be dependent on the excitation power density rather than a constant value. The saturation can be obtained easier when the excitation power density is low (not lower than 221.4 mWcm^{-2}, before this value cannot obtain any saturation).

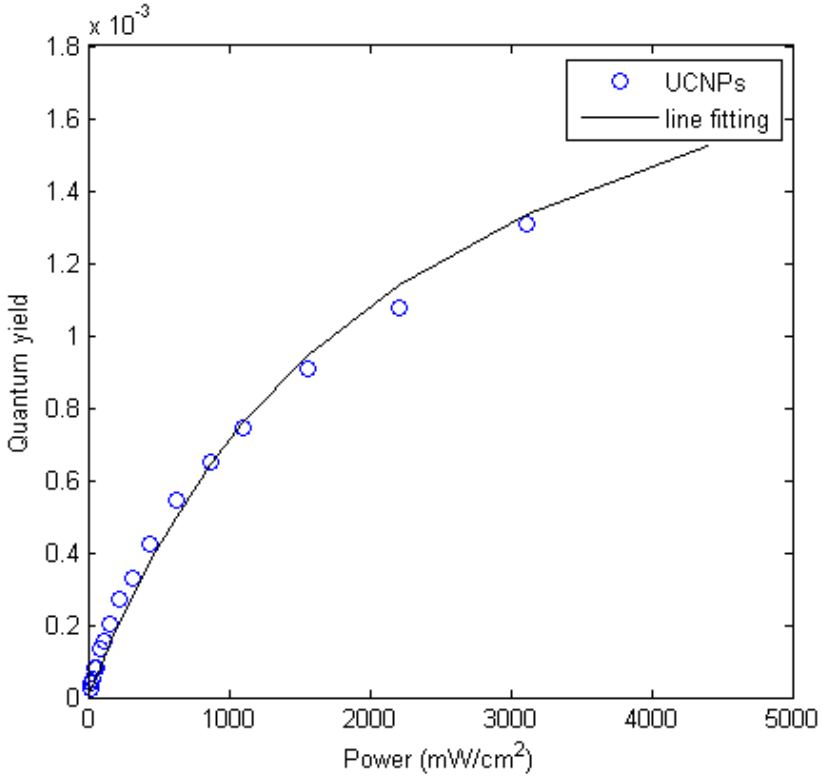

Figure 4.5: Experimentally determined the QY for the $NaYF_4$:Yb^{3+}/Tm^{3+} UCNPs at 800 nm upconversion emission band. The solid black lines are the fitting curves using equation 2.7. Both blue and red dots are measured data, but only blue dots were used for the linear fitting.

The developed setup is very successful in obtaining the saturation of Tm^{3+} particles, since they saturate at low power densities. A curve with slope 2 represents the two-photons excitation process. Increases the power density value, the power dependent upconversion emission curve starts to change, and the slope value decreases. The laser at 975 nm used can only reach maximum power 200 mW, but it provides enough excitation power to demonstrate its strong influence on upconversion. The saturation is used to evaluate the UCNPs QY efficiency; a low saturation power density indicts a high QY. The excitation beam is assumed to have a Gaussian profile, and the beam size is 4.50 mm^2 which is about ten times bigger than the estimation. The beam profiler is calculated based on $\frac{1}{e^2}$ half-width of the beam, which corresponds to 500 pixels in the image recorded by CCD camera. Converting the beam size from pixels to mm gives a diameter of 2.40 mm. During the beam size estimation, the Full-Width Half Maximum (FWHM) was used for the Gaussian beam size measurement. Later during the data analysis, the $\frac{1}{e^2}$ width was used to present the beam size. It is more precise to take the distance between points where the beam intensity falls to $\frac{1}{e^2}$= 13.53% of the maximum intensity instead of the FWHM. This is one of the reasons for the beam size difference between the estimation and experimental data.

The laser power transmission is 85.36% for UCNPs, and the transmission is 77.27% for dye DY-781. The refractive index for cyclohexane is 1.43 and the refractive index for ethanol is 1.36. Where applying equation 2.6 can calculate the luminescence QY of UCNPs, the QY result is plotted in figure 4.5. The experimental QY can be nicely

fitted with equation 2.7 as shown in figure 4.5 with the solid black line. The a value is the estimated maximum attainable QY, it is about 0.23% and the b value is defined as the power density at balance point which equals 2250 $mWcm^{-2}$. The y value is the excitation power density. The discrepancy that the experimental data and line fitting could be due to the excitation laser beam having a uniform cross-section profiler. Based on a paper published by Haichun Liu [35], where the QY is the half of the maximum at balance point, the full QY can be calculated by determining the balance point power density and the corresponding QY, this is how to obtain the value for variable a. In Liu's paper [35], he obtained the balance power density 3800 $mWcm^{-2}$ with 0.45% QY for core $NaYF_4$:Yb^{3+},Tm^{3+} nanoparticles. In this thesis, the balance point has power density 2250 $mWcm^{-2}$ with QY 0.11%. If subtract out the transmission effect from the 800 nm BP filter, the experimental QY value will be 0.33% for nanoparticles, and the balance power density will be 3214 $mWcm^{-2}$. The values for the maximum attainable QY is estimated to be 0.69%. The difference between the QY achieved in this thesis and the QY measured by Haichun is probably due to the UCNPs sample itself. It is unknown if the nanoparticles are expired or polluted, and that was no information about the nanoparticle size either.

There are multiple factors would also affect the measurement. A dirty cuvette would incline the absorption or emission spectrum. Thus, it is very necessary to clean the cuvette. If the cuvette had stored fluorophore before, there is a possibility that the fluorophore is absorbed by the cuvette wall. It is important to use an acid like hydrogen chloride to help clean the cuvette or just use a new cuvette. During the measurement, the 20μM DY-781 solution was too concentrated, its absorbance exceeds the limit 0.05, but this problem can be solved by dilute the fluorophore solution like we performed during the experiment. When there is scattering light in the detection path, this problem can be solved by adding LP and BP filterS, but the addition of filters will lower the luminescence intensity. During the mathematical calculation, it is important to know the transmission rate of filters. Otherwise changing the excitation wavelength can help increase the separation difference between the scattered excitation light and emission light, especially because the DY-781 has a broad emission spectrum. Also, as mentioned above, the excitation beam cross-section profiler affects the QY calculation, it is important to have a stable, perfect Gaussian beam or a stable top-hat laser beam. For the lasers used during this thesis, the excitation power output varies with time; the variation can be obtained from figure 4.1 and figure 4.2. And view the beam profiler at high power; should be noted the beam profiler contains too much noise.

Outlook 5

Although the setup shows promise for relative weak luminescence detection from UCNPs, there are still some factors affecting the measurement. In the future, it is necessary to check the quality of the UCNPs, which can be performed by exciting the UCNPs and the reference dye (with an absolute QY) with same excitation wavelength. It is also important to know the size and morphology of the UCNPs, a transmission electron microscope should be able to examine the particles and provide the information. The biggest challenge during the experiment is that the laser driver is unstable when it is in a certain power range. For the laser with excitation wavelength 785 nm, between power 700 μW to 5.0 mW the laser has strong variation, but when the power value is lower or above that range, the laser is stable. Since the QY is nonlinearly dependent on the excitation power density, the variation of power will cause the variation of detected signal, which will increase the uncertainty of the QY determination. There are two suggestions for solving the laser stability problem.

Two excitation pathways

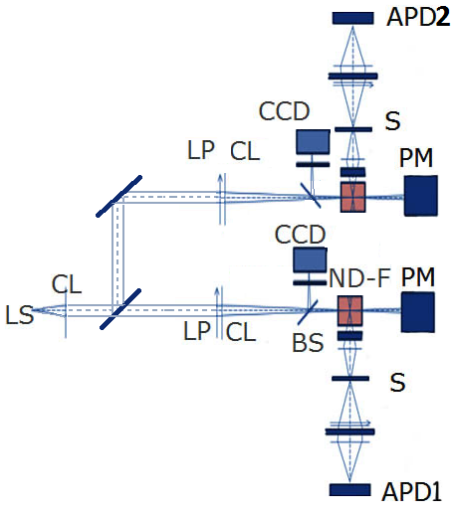

Figure 5.1: The new designed two excitation pathway setup. This setup ensures to record both blank and sample luminescence and transmitted power the same time with the same type of laser beam. Simply subtract the blank cuvette signal data with the sample cuvette signal, can provide the luminescence signal in real time.

Linearly polarized laser light will be split into two beams at the beginning of the excitation path. Two beams will be examined by its individual CCD camera in their excitation path

and be focal into either blank or sample cuvette. Each sample holder has one power meter mounted onto it. Both blank and sample cuvettes have their own but identical luminescence detection path. A program that can record data for two power meters and two APDs the same time should also be developed. Using this setup, it cannot fix the laser stability problem, but it will ensure the same type of laser beams are focal to two different samples the same time. Even there will be laser variation at higher power, but since both power meters and APDs are recording data the same time, during the data evaluation the variation can be easily normalized.

Laser drive stabilization

As mentioned before, the laser drive is unstable when it is in a certain power range. When the laser power is at a very low or a very high value, the laser is stable. Thus, one can set the laser drive always to its maximum power for a stable output, with a reflective ND filter wheel is mounted right after the laser source adapter. It can be manual filter wheel or a motorized filter wheel; the only requirement is it shall contain as many reflective ND filters with different OD values as possible. The excitation power will now depend on the OD values instead of drive current; the laser beam output will stay stable. However, the problem with this setup is, due to filter itself will absorb energy from the beam, so it will be very difficult to achieve a low excitation power. It is not recommended to perform this setup if the lasers used during this thesis work continues to be used. Otherwise, this would be a good approach to investigate the sample with different high excitation power density with a stable laser beam.

Bibliography

[1] Condeelis J, Segall JE. Intravital imaging of cell movement in tumors. Nat. Rev. Cancer 3:921–30 (2013).

[2] Jain RK, Munn LL, Fukumura D. Dissecting tumor pathophysiology using intravital microscopy. Nat. Rev. Cancer 2:266–76 (2002).

[3] Liu HC, Advancing Upconversion Emissions for Biomedical Imaging. Doctoral Thesis, Lund University (2014).

[4] Gao X, Dave SR, Quantum dots for cancer molecular imaging. Adv. Exp. Med. Biol. 620, 57–73 (2007).

[5] Ntziachristos V, Yodh AG, Schnall M, Chance B. Concurrent MRI and diffuse optical tomography of breast after Indochinese green enhancement. Proc. Natl. Acad. Sci. U. S. A. 97, 2767–2772 (2000).

[6] Hoffman RM. The multiple uses of fluorescent proteins to visualize cancer in vivo. Nat. Rev. Cancer 5, 796–806 (2005).

[7] Thomasson B. High accuracy relative luminescence quantum yield measurements of upconverting nanoparticles, Master Thesis, Lund University (2015).

[8] Menter JM. Temperature dependence of collagen fluorescence. Photochem. Photobiol. Sci. 5 (4): 403–410. PMID 16583021 (2006).

[9] F. Auzel. Upconversion and anti-stokes processes with f and d ions in solids. Chem. Rev. 104, 139–173 (2004).

[10] Page RH, Schaffers KI, Waide PA, Tassano JB, Payne SA, Krupke WF, Bischel WK. Upconversion-pumped luminescence efficiency of rare-earth-doped hosts sensitized with trivalent ytterbium. J. Opt. Soc. Am. B 15, 996–1008 (1998).

[11] Cui WN, Ni SY, Shan SN, Zhou XP. A method to improve the up-conversion fluorescence of polymer modified $NaYF_4$: Yb^{3+},Tm^{3+} nanocomposites. Chem. SciRes(2012).

[12] Zhao CZ, Kong XG, Liu XM, Tu LP, Wu F, Zhang YL, Liu K, Zeng QH, Zhang H. Li^+ ion doping: an approach for improving the crystallinity and upconversion emission of $NaYF_4$: Yb^{3+},Tm^{3+} nanoparticles. The Royal Society of Chemistry. (2013).

[13] Lin JH, Liou HY, Wang CD, Tseng CY, Lee CT, Ting CC, Kan HC, Hsu CC. Giant enhancement of Upconversion Fluorescence of $NaYF_4$: Yb^{3+},Tm^{3+} Nanocrystals with resonant waveguide grating substrate. Dep.Phys. ACS Publication. (2015).

[14] Wang L, Liu WP, Liu ZY, Zhao D, Qin GS, Di WH, He CF. Improved 800 nm emission of Tm^{3+} sensitized by Yb^{3+} and Ho^{3+} in $\beta-$ $NAYF_4$ nanocrystals under 980nm excitation.Optic Express 7602.(2012)

[15] Li CX, Quan ZW, Yang J, Yang PP, LinInorg J. Highly Uniform and Monodisperse $\beta-NaYF_4$: Ln^{3+} (Ln=Eu, Tb, Yb/Er, and Yb/Tm)Hexagonal micro prisms crystals: hydrothermal synthesis and luminescent properties.Chem. pp. 6329-6337.(2007)

[16] Chen G, Ohulchanskyy TY, Kumar R, Agren H, and Prasad PN. Ultrasmall monodisperse $NaYF_4$: Yb^{3+},Tm^{3+} nanocrystals with enhanced near-infrared to near-infrared upconversion photoluminescence. ACS Nano 4(6), 3163–3168 (2010).

[17] Chen G, Ohulchanskyy TY, Law WC, Agren H, Prasad PN. Monodisperse NaYbF4: Tm3+/NaGdF4 core/shell nanocrystals with near-infrared to near-infrared upconversion photoluminescence and magnetic resonance properties. Nanoscale 3(5), 2003–2008 (2011).

[18] Dexter DL. A theory of sensitized luminescence in solids. J. Chem.Phys.21, 836–850 (1953).

[19] Feng W, Yu H, Chin SL, Yunhao L, Juan W, Jun X, Hongyu C, Chun Z, Minghui H, Xiaogang L. Simultaneous phase and size control of upconversion nanocrystals through lanthanide doping. Nature 463, 1061-1065 (25 February 2010)

[20] Heer S, Kompe K, Gudel HU, Haase M. Highly efficient multicolor upconversion emission in transparent colloids of lanthanide-doped $NaYF_4$ nanocrystals. Adv. Mater. 16(23–24), 2102–2105 (2004).

[21] Zhang F. Photon upconversion nanomaterials. Department of Chemistry, Fudan University, Shanghai, China. (2015)

[22] Chen G, Yang C, Prasad PN. Nanophotonics and nanochemistry: controlling the excitation dynamics for frequency up- and down-conversion in lanthanide-doped nanoparticles. Acc. Chem. Res. 46, 1474–1486 (2013)

[23] Williams ATR, Winfield SA, Miller JN. Relative fluorescence quantum yields using a computer-controlled luminescence spectrometer, Analyst, 1983, 108, 1067.

[24] Dyomics, "DY-781"[Internet][cited 2016 March 20th] Avaliable from:`http://www.dyomics.com/en/products/nir-excitation/dy-781.html`

[25] PM16-121 USB power meter standard photodiode power sensor[Internet][cited 2016 March 27th] Avaliable from:`https://www.thorlabs.com/thorproduct.cfm?partnumber=PM16-121`

[26] DCU224M-CCD Camera, 1280 x 1024 Resolution, B&W, USB 2.0 [Internet][cited 2016 March 27th] Avaliable from:`https://www.thorlabs.de/thorproduct.cfm?partnumber=DCU224M`

[27] Fiji [Internet] [cited 2016 March 27th] `http://fiji.sc/`

[28] APD410A/M - Si Variable-Gain Avalanche Detector, Temperature Compensated, 400 - 1000 nm, DC - 10 MHz, M4 Taps.[Internet] [cited 2016 March 27th] `https://www.thorlabs.com/thorproduct.cfm?partnumber=APD410A/M`

[29] Xu CT, Svenmarker P, Liu HC, Wu X, Messing E.m, and Andersson-Engels S. High-resolution fluorescence diffuse optical tomography developed with nonlinear upconverting nanoparticles.Phys. ACSNANO.2012.

[30] Maciel S, Biswas A, Kapoor R, Prasad PN. Blue cooperative upconversion in Yb^{3+}-doped multicomponent sol-gel-processed silica glass for three-dimensional display. Prasad, Appl. Phys. Lett., 2000, 76, 1978–1980.

[31] Wang H, Duan C, Tanner PA. J.Visible. Upconversion luminescence from Y2O3: Eu^{3+},Yb^{3+}. Phys. Chem. C, 2008, 112, 16651–16654

[32] Erdogan T. Understanding polarization, semrock white paper series

[33] Quintanilla M., Cantarelli IX., Pedroni M., Speghini A. and Vetrone F. Intense ultraviolet upconversion in water dispersible SrF_2: Tm^{3+},Yb^{3+} nanoparticles: the effect of the environment on light emissions. J. Mater. Chem. C, 2015,3, 3108.

[34] BAM federal institute for materials research and testing, richard-willstätter-Str.11, 12489 Berlin, Germany

[35] Liu HC, Xu CT, Lindgren D, Xie HY, Thomas D, Gundlach C and Andersson-Engels S. Balance power density based quantum yield characterization of upconverting nanoparticles for arbitrary excitation intensities. Nanoscale, 2013, 5, 4770.